



ISSN NO. 2320-5407

Journal homepage: <http://www.journalijar.com>
Journal DOI: [10.21474/IJAR01](https://doi.org/10.21474/IJAR01)

**INTERNATIONAL JOURNAL
OF ADVANCED RESEARCH**

RESEARCH ARTICLE

Study of Sapphire and MgO as Thermal Neutron Filters for The TRIGA Moroccan Reactor Beam ports.

***N. Zahar¹, D. Benchekroun¹, B. Belhorma², P. Hermet³ and C. Broeders⁴.**

1. RUPHE, Hassan II University, Faculty of Sciences, Casablanca, Morocco.
2. National Center for Nuclear Energy, Sciences and Technology, Rabat, Morocco.
3. Institut Charles Gerhardt, Equipe C2M, UMR CNRS 5253 Montpellier, France.
4. Karlsruhe Institute of Technology, Germany.

Manuscript Info

Abstract

Manuscript History:

Received: 12 May 2016
 Final Accepted: 22 June 2016
 Published Online: July 2016

Key words:

Attenuation, sapphire, Geant4
 Thermal Neutrons.

*Corresponding Author

N. Zahar.

We focus on the thermal neutrons interaction with sapphire and MgO crystals that are frequently used as thermal neutron filters. The LEAPR module of NJOY code has been used to generate the thermal neutron cross sections for sapphire and MgO crystals at different temperatures. The phonon density-of-states, required by the LEAPR module, has been calculated using the ABINIT package. The generated cross sections allow us to study the temperature effect on the quality of each filter and to compare the filtering powers of the two considered crystals. Geant4 simulations based on the generated thermal cross section give reasonable transmission rates for sapphire filter at room temperature.

Copy Right, IJAR, 2016,. All rights reserved.

Introduction:

The neutron diffraction for materials study is one of the applications that will be developed around the 2.0 MW TRIGA MARK-II Moroccan research reactor installed at the Moroccan National Center of Nuclear Energy, Sciences and Technics (CNESTEN).

For this application, the neutron beam emerging from the reactor should first be filtered in order to minimize the fast neutrons contribution. Single crystal sapphire (Al_2O_3) is frequently used as fast neutron filter in experiments around research reactors. Several works have also shown that MgO crystal could be a good thermal neutron filter [1,2]. The neutron filter material must have a low cross section for thermal neutrons, with energy less than 0.1 eV, and a high cross section for energies greater than about 1 eV.

Several works on thermal neutrons filters have been already published. Experimental works of Born [3] and Mildner [4,5] have been devoted to the characterization of filters based on sapphire and MgO crystals. It has been shown that at room temperature, sapphire and MgO have similar transmissions and only a small increase in thermal neutron transmission is achieved by cooling the sapphire.

I.E. Stamatelatos and S. Messoloras [6] have published a work on the optimization by simulation of the sapphire filter thickness in the neutron scattering experiments. For fast neutrons, the transmission was calculated using the MCNP code while the thermal cross sections were derived from the Cassels formula [7] due to the absence of the sapphire thermal cross section in the available simulation codes.

More recently, Mishra et al. [8] used a combination of ab-initio calculations with the NJOY code to calculate accurate cross sections for thermal neutrons.

Until now, no database containing thermal cross sections of the most used crystals, such as sapphire and MgO, are available. The simulation of neutron scattering experiments, such as the Moroccan TRIGA reactor beam port, needs the generation of the thermal neutron cross section for the crystals used as thermal neutron filters.

The overall cross section σ_{th} is a superposition of several contributions: (a) absorption, σ_a , proportional to neutron wavelength, (b) inelastic, σ_{inel} and (c) elastic or Bragg scattering, σ_{ela} which depends on neutron wavelength, crystal orientation and crystal perfection. Item (b) depends on crystal temperature (phonon population), where coherent Bragg scattering can be disallowed by using a particular crystal orientation [9]:

$$\sigma_{Th} = \sigma_a + \sigma_{inel} + \sigma_{ela} \quad (1)$$

The maximum efficiency of such filter is given by the optimum filter thickness, the crystal orientation and the temperature.

One can also use the quality factor R, defined by the ratio of the total cross section at thermal energies, σ_{th} , to the total cross section at high energies, σ_{free} :

$$R = \frac{\sigma_{th}}{\sigma_{free}} \quad (2)$$

The absolute minimum value of R is obtained by neglecting σ_{ela} Contribution:

$$R_{min} = \frac{\sigma_a + \sigma_{inel}}{\sigma_{free}} \quad (3)$$

The lower value of R_{min} corresponds to the best filter. A low value for the numerator implies a good transmission of neutrons in the desired thermal energy range, while a large denominator ensures strong scattering of the unwanted epithermal and fast neutrons. The filter also acts to reduce the intensity of any γ -ray beam that accompanies the neutron beam.

Thermal Cross Sections Problematic:

The purpose of the present work is to find the optimal filter thickness that gives good fast neutrons attenuation and high transmission of thermal neutrons using the Geant4 code [10]. The Monte Carlo code Geant4 (geant4.10.01 version) was used to calculate the transmission ratio of fast neutrons for different sapphire crystal thicknesses. Fig. 1 shows the fast neutrons transmission as a function of the crystal thickness L.

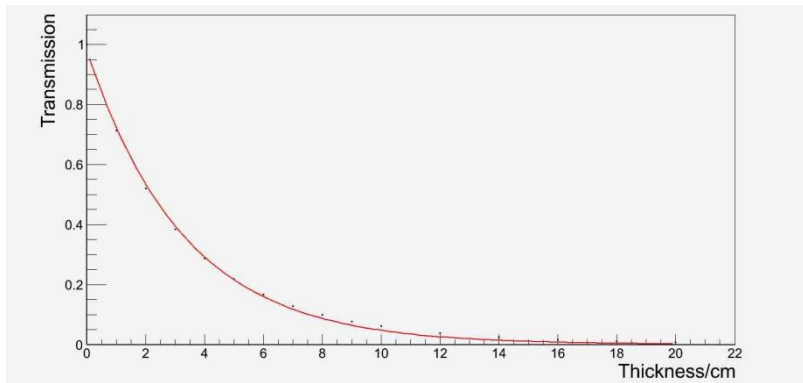


Fig. 1: Fast neutron transmission as a function of sapphire crystal thickness

The calculated neutron transmission can be adjusted by the empirical function:

$$T = I/I_0 = \exp(-L/\lambda) \quad (4)$$

The simulation results give a value of the λ parameter of 33.07 mm. This value compares well with 33.3 mm of ref. [3] and 31.3 mm of ref. [6]. For MgO, Geant4 simulations give a λ parameter of about 36.5 mm.

However, for the same thickness, the calculated transmission rate of thermal neutrons is about 3% which does not suit the purpose of a thermal neutron filter. The reason of this disagreement comes from the thermal cross sections that are not correctly implemented in Geant4 for many materials.

The Geant4 code can treat the physically reliable transport of thermal neutrons if the $S(\alpha, \beta)$ inelastic cross section data are used. In this case, it takes into account atomic translational motion as well as vibration and rotation of the bound atoms that also significantly affect the cross sections and final states. The current G4NDL Thermal Scattering data library contains $S(\alpha, \beta)$ data for some molecules, such as H bounded in ZrH. However, there is no ENDF data library for Al_2O_3 . The main task of the next steps is to generate thermal scattering data for the Al_2O_3 and MgO crystals to incorporate them in the GEANT4 database.

Thermal Neutron Scattering cross sections:

The calculation of thermal neutron scattering cross sections in such materials requires information on the absorption and inelastic scattering since the elastic scattering is neglected. The inelastic scattering cross sections are calculated by using NJOY code [11]. The phonon frequency distribution, generated independently by ab-initio calculations, is the main input for accurate thermal cross sections determination at various temperatures.

Phonon frequency generation for sapphire and MgO:

Born effective charge tensor and dynamical matrices of Al_2O_3 and MgO were computed within a variational approach to density functional perturbation theory as implemented in the ABINIT package [12]. The exchange-correlation energy functional was evaluated within the generalized gradient approximation according to Perdew, Burke and Ernzerhof scheme [13]. $\text{Al}(3s^2, 3p^1)$, $\text{Mg}(3s^2)$ and $\text{O}(2s^2, 2p^4)$ -electrons were considered as valence states in the construction of the pseudopotentials. The electronic wavefunctions were expanded in plane-waves up to a kinetic energy cutoff of 57 Ha. Integrals over the Brillouin zone were approximated by sums over a $8 \times 8 \times 8$ mesh of special k-points [14]. Atomic positions of each structure were relaxed at their corresponding experimental volume and lattice parameters: rhombohedral unit cell belonging to the $R\bar{3}c$ space group with $a = 5.128 \text{ \AA}$ and $\alpha = 55.28^\circ$ for Al_2O_3 [15], and cubic unit cell belonging to the $Fm\bar{3}M$ space group with $a = 2.979 \text{ \AA}$ and $\alpha = 60^\circ$ for MgO [16]. Phonon dispersion curves were interpolated according to the scheme described in ref [17]. In this scheme, the long-range character of the dipole-dipole contribution is correctly handled by first subtracting it from the force constant matrix in reciprocal space and treating it separately. The short-range contribution to the interatomic force constants in real space is then obtained from the remainder of the force constant matrix in q-space using a discrete Fourier transform. From the resulting set of interatomic force constants in real space, phonons can be readily obtained at any point in the Brillouin zone. For the both materials, a $150 \times 150 \times 150$ q-points grid in the irreducible Brillouin zone was employed for the calculation of the integrals associated with the phonon density-of-states. They are displayed in Figs.2 respectively for Al_2O_3 and MgO.

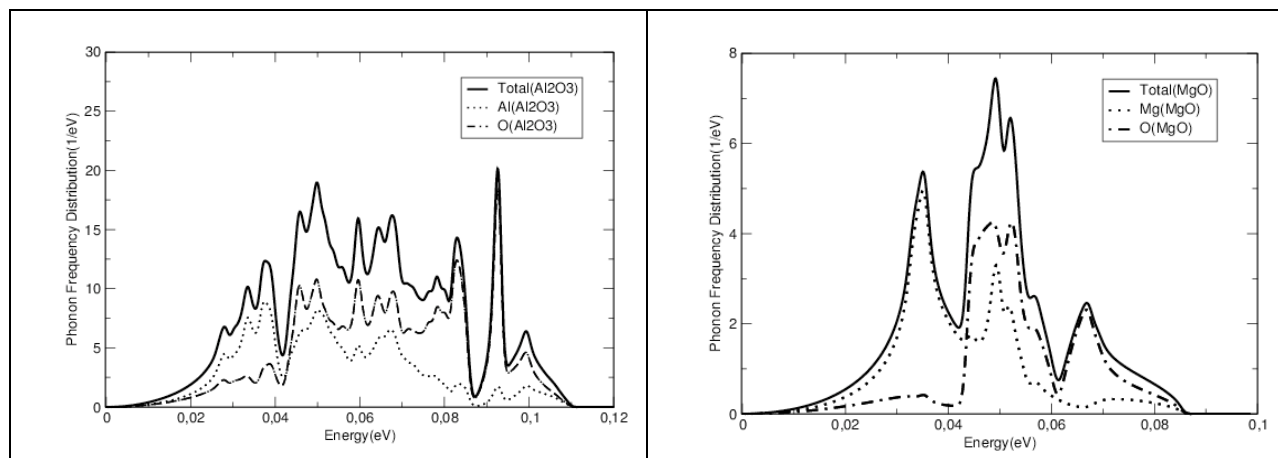


Fig. 2: Partial and total phonon frequency distributions for Al_2O_3 (left) and MgO (right)

Thermal inelastic cross section:

The calculation of inelastic cross section, based on the $S(\alpha, \beta)$ model, was handled by LEAPR module of the NJOY tool at different temperatures. The double differential cross section for thermal neutrons is given by [11,18]:

$$\frac{\partial^2 \sigma(E \rightarrow E', \mu)}{\partial E \partial \mu} = \frac{\sigma_b}{2kT} S(\alpha, \beta) \quad (5)$$

E and E' are the incident and outgoing neutron energies, μ is the cosine of the scattering angle in the laboratory system, σ_b is the characteristic bound scattering cross section for the material and kT is the thermal energy in eV. $S(\alpha, \beta)$ is the asymmetric form for the scattering law, defined as a function of the momentum transfer α and the energy transfer β . In the case of the incoherent and Gaussian approximations, the scattering law $S(\alpha, \beta)$ can be written as a function of $\rho(\beta)$, the frequency spectrum of excitations in the system :

$$S(\alpha, \beta) = \frac{1}{2\pi} \int_{-\infty}^{+\infty} E^{i\beta\hat{t}} E^{-\gamma(\hat{t})} d\hat{t} \quad (6)$$

\hat{t} is the time expressed in units of $\hbar/(kT)$. The function $\gamma(\hat{t})$ is given by:

$$\gamma(\hat{t}) = \alpha \int_{-\infty}^{+\infty} \frac{\rho(\beta)}{2\beta \sinh(\beta/2)} (1 - e^{-i\beta\hat{t}}) e^{-\beta/2} d\beta \quad (7)$$

Fig. 3 shows the total neutron cross section per sapphire molecule at room temperature (300 K). The results are in a good agreement with experimental data from the Nuclear Reaction Data base [19] and with the results of Mishra et al. [8].

The cross section distribution has a minimum around $E = 0.025$ eV which could ensure a good transmission of thermal neutrons. For higher energies, the cross sections are compatible with those derived from the free-atom assumption. The cross section distributions for sapphire and MgO are similar; except the absorption contribution to the total cross section which is lower in the case of MgO crystal [20] (σ_a for magnesium is much smaller than for aluminium).

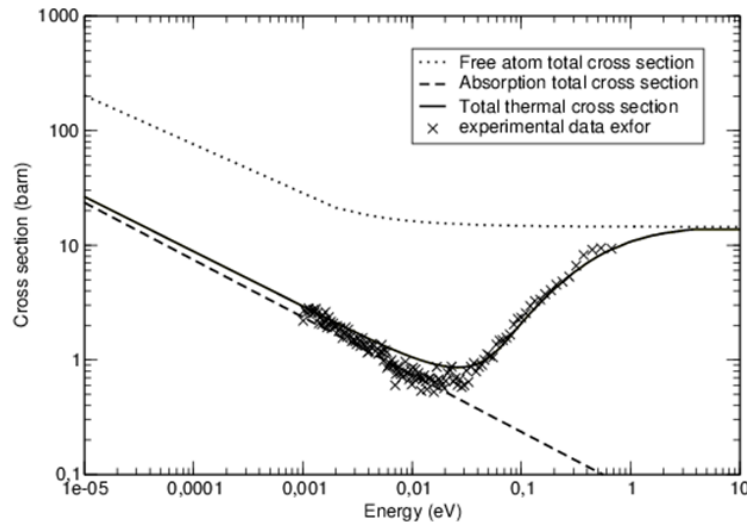


Fig. 3: Total cross section per molecule for sapphire crystal at 300 K.

In Fig. 4 are compared the total cross sections for sapphire and MgO at room and liquid nitrogen temperatures (300 K and 77 K). The filter quality is considerably improved by cooling the crystal. The real effect of the temperature on the filter quality will be discussed in the next section.

Results and Discussion:

To show the effect of cooling on the ability of sapphire Al_2O_3 and magnesium Oxide MgO filters to attenuate fast, epithermal neutrons and transmit thermal neutrons, the quality factors R were calculated at room and liquid nitrogen temperatures. Tables I and II list respectively R_{min} for sapphire and MgO filter materials at both temperatures. The values of R_{min} for sapphire compare well with experimental results at 300 K. At both temperatures, the MgO filter

seems to have a slightly better quality than sapphire filter. Also, the improvement of the quality factor R by the crystal cooling is higher for MgO than for Al_2O_3 .

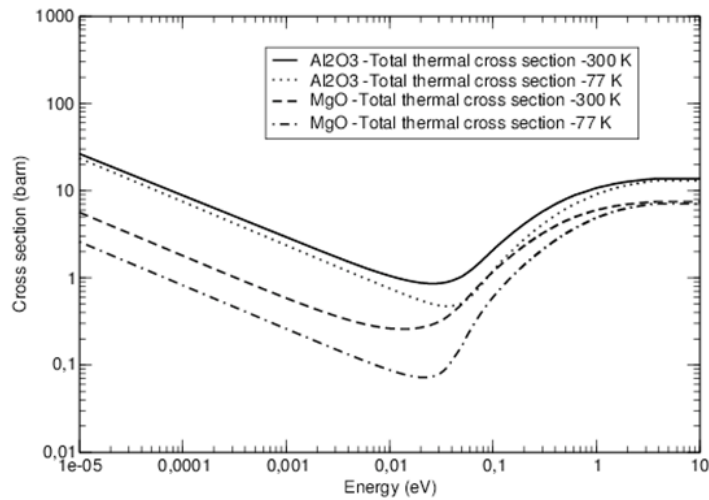


Fig. 4: Comparison of the Total cross section per molecule for MgO and sapphire crystals at 300 K and 77 K.

Table I : R_{\min} for Al_2O_3 compared to experimental values from [3]

Energy (ev)	Al_2O_3		
	R_{\min} [300 K]	R_{exp} [300K]	R_{\min} [77 K]
0.014	0.0600	0.07	0.0408
0.034	0.058	0.06	0.0335
0.057	0.08	0.1	0.6283
0.1344	0.2	0.33	0.8691

Table II : Quality factor R_{\min} for MgO

Energy (ev)	MgO	
	R_{\min} [300 K]	R_{\min} [77 K]
0.014	0.032	0.01
0.034	0.044	0.012
0.057	0.077	0.03
0.1344	0.21	0.12

The transmission rate can be calculated using the formula:

$$T_n = \frac{I_x}{I_0} = e^{-n\sigma_n x} \quad (8)$$

σ_n = total cross section calculated by the NJOY code,
 n = number of molecules per volume unit and
 x = crystal thickness.

The optimal filter thickness must allow a good absorption of fast neutrons while keeping a high fraction of incident thermal neutrons. In the real situation, the thermal and fast neutron fluxes emerging from the reactor are not equal. Thus, we can use the quality factor Q given by [4]:

$$Q = A(T_{\text{Th}}(E_n, L) - \alpha T_f(L)) \quad (9)$$

T_{th} and T_f denote respectively the transmission rates for thermal and fast neutrons, calculated using Eq. (8).

The α factor takes into account the ratio of thermal and fast neutrons intensities emerging from the reactor ($\alpha \leq 1$). The worst case corresponds to $\alpha = 1$.

Figures 5 and 6 show the quality factor Q as a function of the filter thickness, for sapphire and MgO crystals respectively ($T = 300$ K). For both crystals, a maximum around 7 cm is observed for $\alpha = 1$, the maximum is more apparent for a more realistic value of α ($\alpha = 0.5$). For both crystals, the optimal thickness is around 7 cm. The corresponding transmission rate is about 87 % for sapphire and 89 % for MgO, for 0.025 eV neutrons. While the fast neutrons transmission rate is about 12 % for sapphire and 15 % for MgO. These results are in agreement with those of R. Born et al. [3] and N. Habib [9].

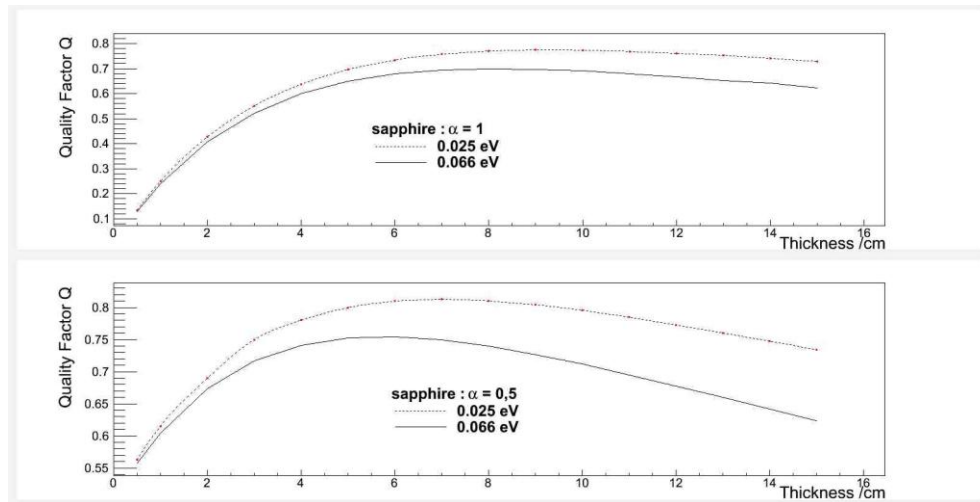


Fig. 5: Quality factor Q for sapphire as a function of the crystal thickness

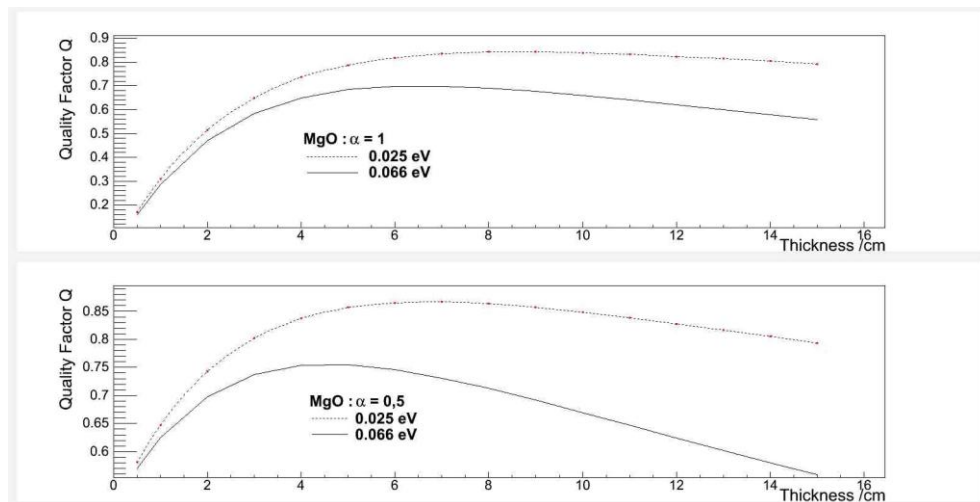


Fig. 6: Quality factor Q for MgO as a function of the crystal thickness

In Figure 7 is given the comparison of sapphire and MgO transmission rates at 300 K and 77 K, obtained with a crystal thickness of 7 cm. At 300 K, we observe a higher transmission for sapphire at fast energies but a much deeper transmission window at thermal energies for MgO, which is in agreement with the results of Mildner et al. [4,5].

At liquid nitrogen temperature (77 K), the best transmission rate is achieved with MgO crystal, which shows that cooled MgO crystals are better than sapphire for the transmission of long wavelength neutrons. The transmission curves for MgO are in agreement with the results found by Adib et al. [1].

The comparison of the transmission rates 300 K and 77 K, for $E_n < 0.02$ eV, show that only a small increase $\approx 5\%$ is achieved by cooling the sapphire crystal at 77 K. Such a small increase could be insufficient to warrant the expense of cryogenics. The same conclusions have been done experimentally by Mildner et al. [4,5].

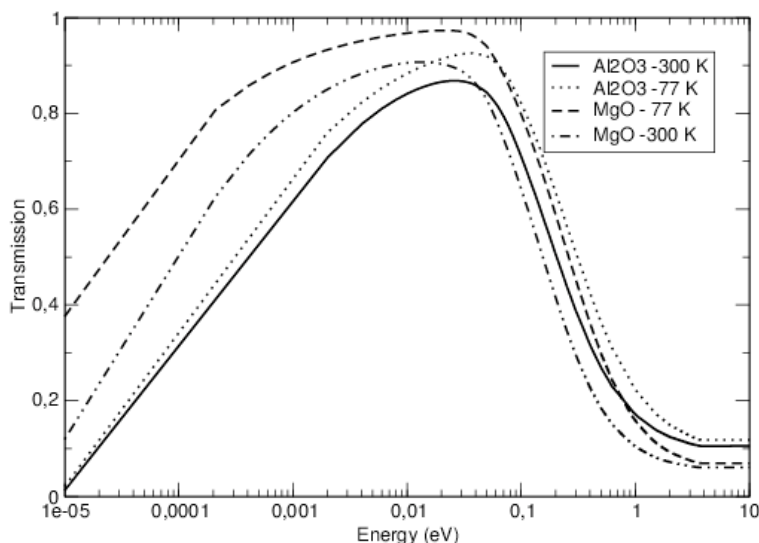


Fig.7: Neutron transmission through 7 cm MgO and Al_2O_3 Crystals at 300 K and 77 K, as a function of neutron energy.

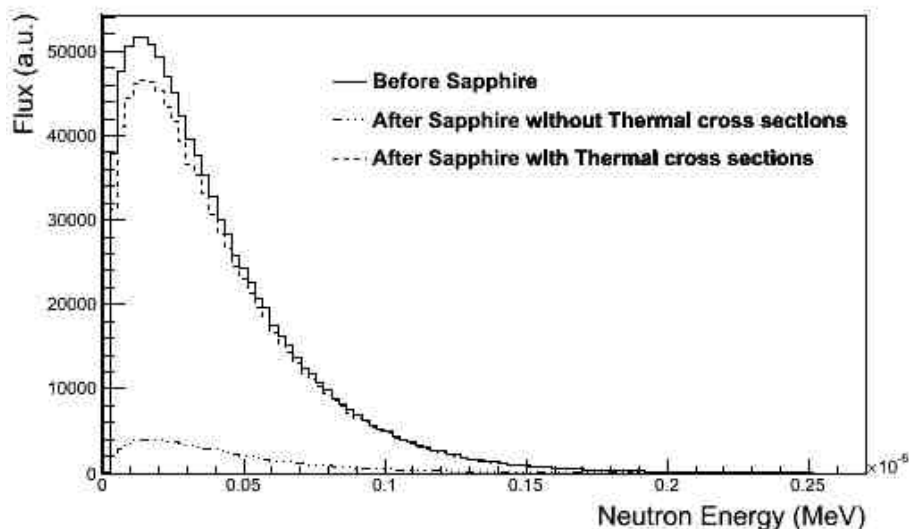


Fig. 8: Leakage neutron spectrum, from Geant4 simulation, obtained with and without thermal cross sections compared to the incident Neutron spectrum.

The cooling the MgO crystal at 77 K improves significantly the thermal transmission. An increase of about 20% can be achieved for long-waved neutrons.

The thermal cross sections for sapphire at 300 K have been translated to the G4NDL format. Geant4 simulations (geant4.10.01) have been performed starting with a Maxwell-Boltzman thermal neutron spectrum, incident on a 7 cm thick sapphire filter. Figure 8 shows the transmitted neutrons spectrum obtained using the standard Geant4 cross

sections (free atoms approximation) and with the thermal cross sections.

A drastic reduction of the thermal neutron flux is observed when free atoms cross sections are used, whereas a good transmission is obtained after an appropriate modeling of thermal neutrons interactions. In this case, an integrated transmission of about 90% is achieved through a 7 cm thick sapphire filter.

Conclusion:

The thermal neutron cross sections have been generated by the NJOY code to estimate the transmission of thermal and fast neutrons through sapphire and MgO crystals. The cross sections generation based on the $S(\alpha, \beta)$ model is a long procedure beginning from ab-initio calculation of the phonon spectrum and leading to a cross section distribution to be validated by experimental data. The obtained cross sections can be used to estimate the quality of each filter at different temperatures.

The results show that, at room temperature, MgO filter has a slightly better thermal transmission than the sapphire filter. The cooling of the crystal at liquid nitrogen temperature improves significantly the filtering quality of the MgO filter while the gain for sapphire does not justify the cost of cooling.

Finally, accurate Geant4 simulations, using the validated thermal cross section, show a good transmission in the thermal region. Unlike the use of the free atoms approximation that leads to a dramatic reduction of the thermal transmission.

The authors would like to thank Tatsumi Koi, member of the GEANT4 collaboration group, for his help for the cross sections translation to the G4NDL format.

This work is supported by the Moroccan High Energy Physics Network (RUPHE).

References:

1. **Adib et al.**, Annals of Nuclear Energy 38 (2011) 2673-2679.
2. **P. Thiyagarajan et al.**, J. Appl. Cryst. (1998) 31, 841-844.
3. **R. Born et al.** Nucl. Inst. And Meth. In Phys. Res. A262 (1987) 359-365.
4. **D.F.R. Mildner et al.**, J. Appl. Cryst. (1993) 26, 438-447.
5. **D.F.R. Mildner and G.P. Lamaze**, J. Appl. Cryst. (1998) 31, 835-840.
6. **I.E. Stamatelatos and S. Messoloras**, Rev. Sci. Instrum. 71, 70.73, January (2000).
7. **J.M. Cassels**, Prog. Nucl. Phys. 1, 185 (1950).
8. **Kaushal K. Mishra et al.** IEEE Transactions on Nuclear Science, Vol. 53, No. 6 (2006).
9. **N. Habib**, Single crystal Filters for neutron spectrometry, Presented at the 2007 6 th Conference on Nuclear and Particle Physics, Luxor, Egypt. Nov 17-21, 2007.
10. **Geant 4 Collaboration**, Nucl. Inst. And Meth. In Phys. Res.,
11. A506 (2003) 250-303.
12. **R. E. Macfarlane, D. W. Muir, R. M Boicourt and A. C. Kahler**, "The NJOY Nuclear Data Processing System, Version 2012," LA-UR-12-27079, Los Alamos National Laboratory
13. **X. Gonze et al.**, Comput. Phys. Comm. (2009) 180, 2582-2615.
14. **J. P. Perdew, K. Burke, M. Ernzerhof**, Phys. Rev. Lett. (1996) 77, 3865.
15. **H. J. Monkhorst, J.D. Pack**, Phys. Rev. B (1976) 13, 5188-5192.
16. **P. Villars**, Pearson Handbook: Crystallographic Data for Intermetallic Phases, ASM International, Materials Park, 1997.
17. **N. W. Ashcroft and N. D. Mermin**, Solid State Physics, Saunders, 1976.
18. **X. Gonze, J.-C. Charlier, D. C. Allan, M. P. Teter**, Phys. Rev. B (1994) 50, 13035-13038.
19. **M. Mattes and J. Keinert**, IAEA report INDC (NDS)-0470, April 2005.
20. **EXFOR database** :<http://www-nds.iaea.org/exfor/exfor.htm>
21. **N. Zahar et al.**, ANIMMA 2013, Marseille – France, 23-27, June 2013.
22. DOI : 10.1109/ANIMMA.2013.6728049